Population Pharmacokinetic Modeling of Oxcarbazepine and its Active Metabolite 10-Monohydroxy Derivative to Inform Dosing in Children with Obesity

Electronic Supplementary Material 1

Clinical Pharmacokinetics

Jaydeep Sinha, B.Pharm, M.Pharm, PhD[1], Kanecia Zimmerman, MD, PhD, MPH[2,3], Stephen J. Balevic, MD, PhD, MPH[2,3,4], Chi Hornik, PharmD[2,3], William J. Muller, MD, PhD[5], Mobeen Rathore, MD[6], Marisa Meyer, DO[7,8]; Yaron Finkelstein, MD[9], Amira Al-Uzri, MD[10], Arpita Lakhotia, MBBS[11]; Stuart Goldstein, MD[12]; Jia-Yuh Chen, PhD[13], Ravinder Anand, MS, PhD[13], and Daniel Gonzalez, PharmD, PhD[3,4] on behalf of the Best Pharmaceuticals for Children Act – Pediatric Trials Network Steering Committee

[1]Department of Pediatrics, UNC School of Medicine, The University of North Carolina at Chapel Hill, Chapel Hill, NC, USA (at the time of performing this work); [2]Department of Pediatrics, Duke University School of Medicine, Durham, NC, USA; [3]Duke Clinical Research Institute, Durham, NC, USA; [4]Department of Medicine, Duke University School of Medicine, Durham, NC, USA; [5]Ann & Robert H. Lurie Children's Hospital of Chicago, Chicago, IL, USA; [6]University of Florida Center for HIV/AIDS Research, Education and Service (UF CARES), Jacksonville Shands Medical Center, Jacksonville, FL, US; [7]Division of Critical Care, Department of Pediatrics, Nemours Children's Hospital, Wilmington, DE, USA; [8]Department of Pediatrics, Sidney Kimmel Medical College at Thomas Jefferson University, Philadelphia, PA, USA; [9]The Hospital for Sick Children, Toronto, Ontario, Canada; [10]Oregon Health and Science University, Portland, OR, USA; [11]University of Louisville Norton Children's Medical Group,

Louisville, KY, USA; [12]Cincinnati Children's Hospital Medical Center, Cincinnati, OH, USA;

[13]The Emmes Company, LLC, Rockville, MD, USA.

Address correspondence to: Daniel Gonzalez, Duke Clinical Research Institute, PO Box 17969, Durham, NC, 27715; daniel.gonzalez@duke.edu.

Supplementary Materials

Contents

1. Supplementary Methods

1.1 Sample collection and bioanalysis

Depending on the participants' age, a 0.2-3 mL blood sample was collected in K_2EDTA Vacutainer (for infants and children) or Microtainer (for neonates), which were allowed to store in ice for a maximum of 30 minutes, if immediate plasma separation was not possible. Plasma was separated by centrifugation (2000 g) at 4 °C and was pipetted into polypropylene cryovials for storage. The cryovials containing plasma were stored at < -70 °C (or < -20 °C for up to maximum 8 h if < -70 °C freezer was not immediately accessible) and were shipped frozen on dry ice to the bioanalytical facility. The analytes were extracted from the plasma by protein precipitation, and reversed-phase HPLC separation was performed using Phenomenex, Synergi 4μm Max-RP, (50 x 2.0 mm, 80 Å) column and a gradient separation method involving mobile phase A (water containing 0.1% [v/v] formic acid) and mobile phase B (methanol:acetonitrile (50:50, v/v) containing 0.1% [v/v] formic acid). Mass spectrometry was done using a Sciex API 6500 system. The lower limit of quantification (LLOQ) for both OXZ and MHD was 1 ng/mL. Acceptable intra- and inter-run accuracy and precision (i.e., ±15% for nominal concentrations and ±20% for LLOQ) were established over the entire concentration range of 1 – 1000 ng/mL that was used for the working standards. Adequate linearity (R^2>0.98) was confirmed between 1-1000 ng/mL for both OXZ and MHD, and their overall recovery in the quality control (QC) samples (3, 150 and 750 ng/mL) were 98.2% and 98.9% respectively. Dilution integrity (for analyzing concentrations above the upper limit of quantification (ULOQ) of 1000 ng/mL) was ensured by validating the method for 50-, 100-, and 150-fold dilution of three higher QC samples of 37500 ng/mL, 75000 ng/mL and 113000 ng/mL respectively with blank human plasma. The method was also validated for short-term bench-top plasma stability (up to 6 h at room

temperature), whole blood stability for 2 h (at room temperature and 4 °C), freeze-thaw stability (from -20 °C and -70 °C to room temperature for up to three cycles), and long-term storage stability in human plasma (at -20 °C and -70 °C) for both the analytes.

1.2 Fat-free mass (FFM) calculation

$$FFM\ (male) = \frac{9270 \times WT}{6680 + 216 \times BMI}$$

Eq. S1 Fat-free mass prediction equation for adult males (18 ≤ PNA < 21 years) [1]

$$FFM\ (female) = \frac{9270 \times WT}{8780 + 244 \times BMI}$$

Eq. S2 Fat-free mass prediction equation for adult females (18 ≤ PNA < 21 years) [1]

$$FFM\ (male\ child) = \left(0.88 + \frac{0.12}{\left[1 + \left(\frac{PNA}{13.4}\right)^{-12.7}\right]}\right) \times \frac{9270 \times WT}{6680 + 216 \times BMI}$$

Eq. S3 Fat-free mass prediction equation for male children (3 ≤ PNA < 18 years) [2]

$$FFM\ (female\ child) = \left(1.11 + \frac{0.11}{\left[1 + \left(\frac{PNA}{7.1}\right)^{-1.1}\right]}\right) \times \frac{9270 \times WT}{8780 + 244 \times BMI}$$

Eq. S4 Fat-free mass prediction equation for female children (3 ≤ PNA < 18 years) [2]

BMI, body mass index (kg/m2); FFM, fat-free mass (kg); PNA, postnatal age (years); WT, total body weight (kg).

1.3 Virtual population for simulation

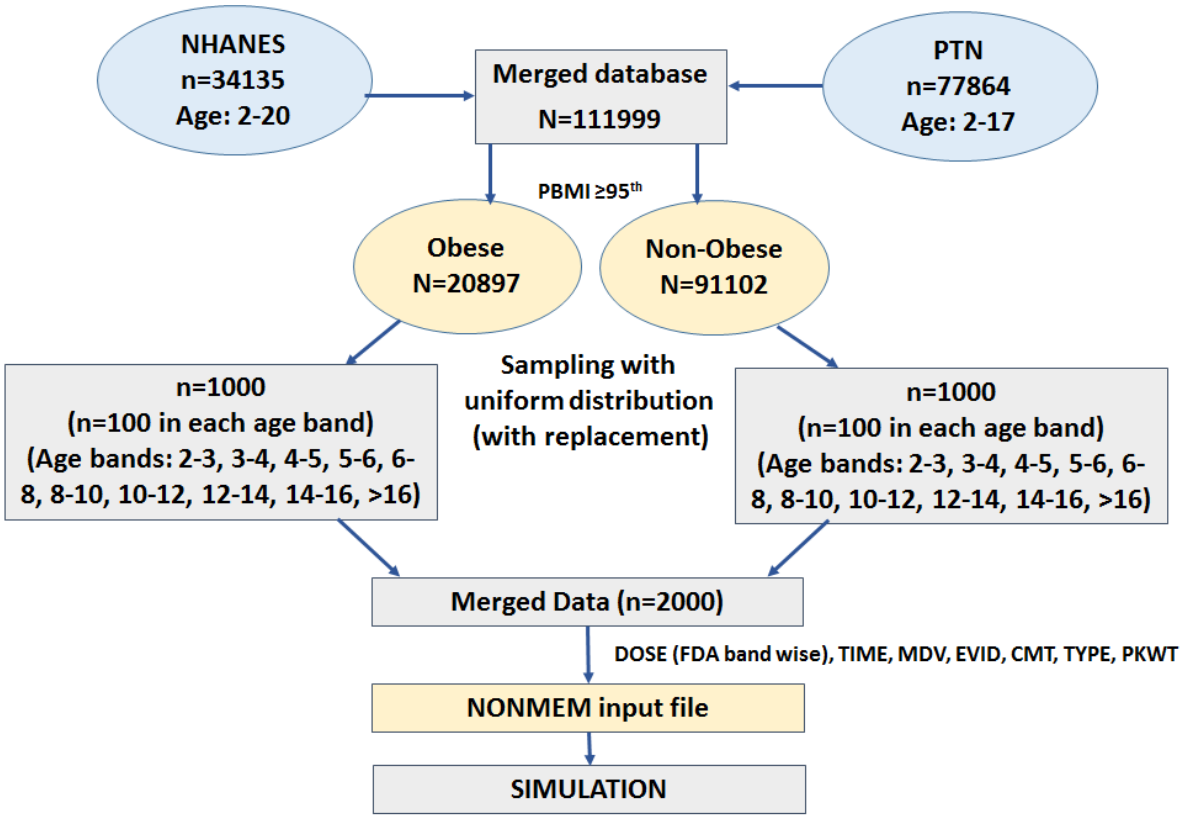

Figure S1. Flow chart of the virtual cohort generation for the simulations.

NHANES, National Health and Nutrition Examination Survey demographic database [3]; PBMI, BMI percentile; PTN, Pediatric Trial Network demographic data repository [4]. DOSE Dosing records (AMT) were added based on FDA recommended age and body weight bands in TRILEPTAL® prescribing information.

2. Supplementary Results

2.1 Concentration vs. time data for the population pharmacokinetic modeling

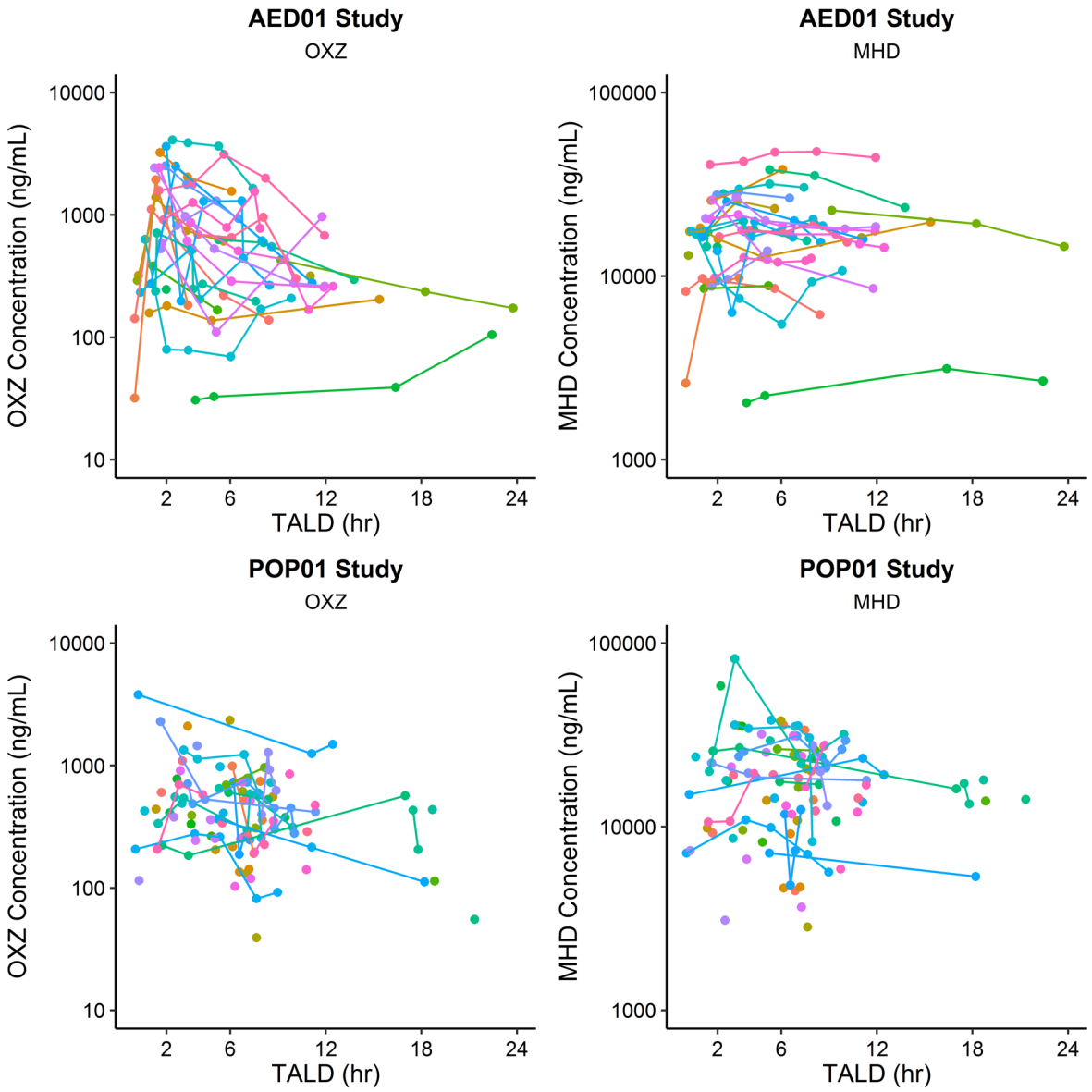

Figure S2. Observed concentration-time profiles from two separate studies.

TALD, time after last dose. Data of oxcarbazepine (OXZ) and its active metabolite 10-monohydroxy derivative (MHD) are shown for AED01 (upper panel) and POP01 (lower panel) studies. Different colors represent different individuals.

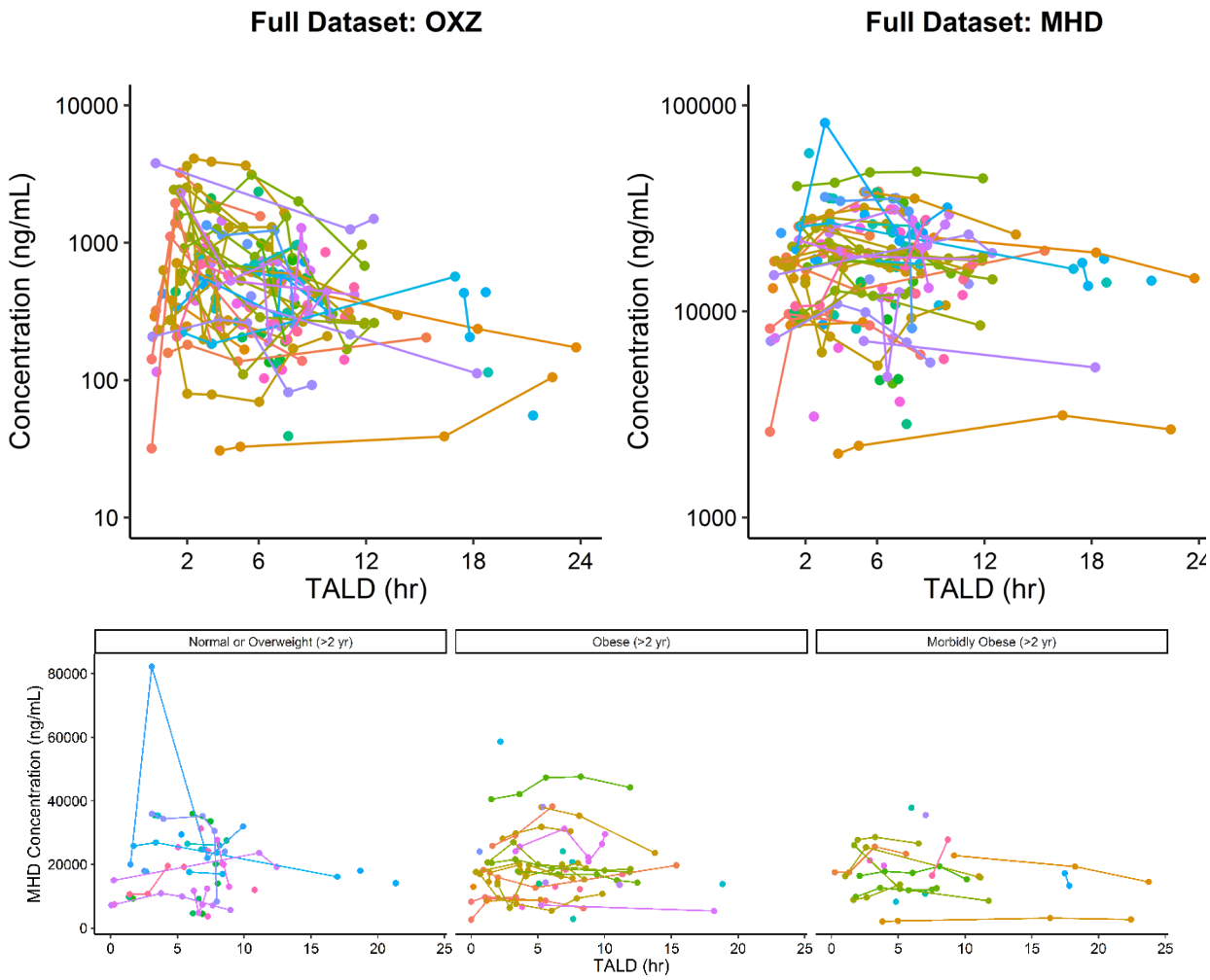

Figure S3. Observed concentration-time profiles of the pooled dataset, which includes POP01 and AED01 study data.

TALD, time after last dose. The upper panel shows the data oxcarbazepine (OXZ) and its metabolite 10-monoydroxy derivative (MHD) for all participants together in the pooled dataset, whereas the lower panel shows the MHD data in three sub-populations of children >2 years of age based on obesity status. Different colors represent different individuals.

2.2 Model development

Table S1. Summary of selection of the structural model.

Model	Ref	K_{bt}	Fixed effects		Random effects fixed	AIC	AIC reduced?	Plausibility of estimates	Comment
			Volume of distribution(L)	Clearance(L/h)					
M1	-	No	$V_{OXZ} = 20$ $V_{MHD} = 20$ $\theta_{V,OXZ} = 0.75^f$ $\theta_{V,MHD} = 0.75^f$	$CL_{OXZ} = 133$ $CL_{MHD} = 2.75$ $\theta_{CL,OXZ} = 0.89$ $\theta_{CL,MHD} = 0.54$	-	6706.89	-	No	• Large ω_{Ka}, $\omega_{V,OXZ}$ • High shrinkage on $\omega_{V,OXZ}$ and $\omega_{V,MHD}$ • Unrealistic RSE (~0%)
M1a	M1	Yes	$V_{OXZ} = 125$ $V_{MHD} = 30.2$ $\theta_{V,OXZ} = 0.75^f$ $\theta_{V,MHD} = 0.75^f$	$CL_{OXZ} = 216$ $CL_{MHD} = 2.76$ $\theta_{CL,OXZ} = 0.89$ $\theta_{CL,MHD} = 0.54$	-	6674.23	Yes	No	• Large ω_{Ka} • High shrinkage on $\omega_{V,OXZ}$ • Unrealistic RSE (~0%)
M1b	M1 a	Yes	$V_{OXZ} = 39.7$ $V_{MHD} = 50.3$ $\theta_{V,OXZ} = 0.75^f$ $\theta_{V,MHD} = 0.75^f$	$CL_{OXZ} = 220$ $CL_{MHD} = 2.81$ $\theta_{CL,OXZ} = 0.91$ $\theta_{CL,MHD} = 0.54$	$\omega_{Ka} = 0$	6711.73	No	Yes	• High shrinkage on $\omega_{V,OXZ}$ • Negligible ω_{Kbt} (~0%)
M1c	M1 b	Yes	$V_{OXZ} = 33.7$ $V_{MHD} = 40.7$ $\theta_{V,OXZ} = 0.75^f$ $\theta_{V,MHD} = 0.75^f$	$CL_{OXZ} = 184$ $CL_{MHD} = 2.84$ $\theta_{CL,OXZ} = 0.89$ $\theta_{CL,MHD} = 0.54$	$\omega_{Ka} = 0$ $\omega_{Kbt} = 0$	6707.52	Yes	Yes	• Large $\omega_{V,MHD}$ • High shrinkage on $\omega_{V,OXZ}$

AIC, Akaike information criteria; CL, clearance of OXZ and MHD (as subscript); f, fixed value; Ka, First order rate constant for absorption; Kbt, First order rate constant for back-transformation; θ, exponent of respective parameter mentioned in subscript;; RSE, relative standard error; V, Volume of distribution of OXZ and MHD (as subscript); ω, between-subject variability of the respective parameter in subscript.

Table S2. Summary of selection of the residual error model.

Model	Ref	Additive error (ng/mL)		Proportional error (CV%)		Random effects fixed	AIC	AIC reduced?	Plausibility of estimates	Comment
		OXZ	MHD	OXZ	MHD					
M1c	-	41.8	705	50.3%	22.5%	$\omega_{Ka} = 0$ $\omega_{Kbt} = 0$	6707.52	-	Yes	• Large $\omega_{V,MHD}$ (97%) • High shrinkage on $\omega_{V,OXZ}$
M1d	M1c	39.5		50.3%	23.2%	$\omega_{Ka} = 0$ $\omega_{Kbt} = 0$	6706.20	Yes	Yes	• Large $\omega_{V,MHD}$ (97%) • High shrinkage on $\omega_{V,OXZ}$
M1e	M1c	No		51.5%	24%	$\omega_{Ka} = 0$ $\omega_{Kbt} = 0$	6707.7	No	Yes	• $\omega_{V,MHD}$ decreased (81%) • $\omega_{V,OXZ}$ also decreased (45%) • High shrinkage on $\omega_{V,OXZ}$
M2	M1e	No		51.6%	24.1%	$\omega_{Ka} = 0$ $\omega_{Kbt} = 0$ $\omega_{V,OXZ} = 0$	6705.83	Yes	Yes	• All reasonable

AIC, Akaike information criteria; CV, Coefficient of variation; ω_{Ka}, ω_{Kbt}, BSV of absorption rate constant and back-transformation constant; $\omega_{V,OXZ}$, $\omega_{V,MHD}$, Between-subject variability (BSV) of volume of distribution of OXZ and MHD respectively.

Table S3. Summary of selection of the scaler from WT and PKWT.

Model	Ref	PK scaler	Changes from the reference model	Fixed effects		AIC	AIC reduced?	Plausibility of estimates	Comment
				Volume of distribution (L)	Clearance (L/h)				
M2	-	WT	-	$V_{OXZ} = 30.5$ $V_{MHD} = 48.6$ $\theta_{V,OXZ} = 0.75^f$ $\theta_{V,MHD} = 0.75^f$	$CL_{OXZ} = 205$ $CL_{MHD} = 2.83$ $\theta_{CL,OXZ} = 0.90$ $\theta_{CL,MHD} = 0.54$	6705.83	-	Yes	• All reasonable
M2a	M2	WT	Volume exponents estimated separately	$V_{OXZ} = 25.4$ $V_{MHD} = 40$ $\theta_{V,OXZ} = 0.64$ $\theta_{V,MHD} = 0.71$	$CL_{OXZ} = 180$ $CL_{MHD} = 2.85$ $\theta_{CL,OXZ} = 0.90$ $\theta_{CL,MHD} = 0.54$	6707.6	No	Yes	• Unrealistic (very high) RSE for all estimates • $\omega_{V,MHD}$ increased to 97%
M3	M2	WT	Volume exponents estimated as a shared parameter between OXZ and MHD	$V_{OXZ} = 26.2$ $V_{MHD} = 39.8$ $\theta_{V,OXZ} = \theta_{V,MHD} = 0.70$	$CL_{OXZ} = 180$ $CL_{MHD} = 2.85$ $\theta_{CL,OXZ} = 0.87$ $\theta_{CL,MHD} = 0.54$	6705.62	Yes	Yes	• High $\omega_{V,MHD}$ (97%)
M3a	M2	WT	Volume exponents fixed to 1 (i.e., linear scaling)	$V_{OXZ} = 31.3$ $V_{MHD} = 67.3$ $\theta_{V,OXZ} = 1^f$ $\theta_{V,MHD} = 1^f$	$CL_{OXZ} = 225$ $CL_{MHD} = 2.78$ $\theta_{CL,OXZ} = 1$ $\theta_{CL,MHD} = 0.53$	6709.85	No	Yes	• Unrealistic (0%) RSE for all estimates

AIC, Akaike information criteria; CL, clearance of OXZ and MHD (as subscript); f, fixed value; θ, exponent of respective parameter mentioned in subscript; RSE, relative standard error; V, volume of distribution of OXZ and MHD (as subscript); ω, between-subject variability of the respective parameter in subscript; WT, total body weight.

Table S3 (continued). Summary of selection of the scaler from WT and PKWT.

Model	Ref	PK scaler	Changes from the reference model	Fixed effects		AIC	AIC reduced?	Plausibility of estimates	Comment
				Volume of distribution (L)	Clearance (L/h)				
M3b	M3	WT (Volume), PKWT (CL)	CL scaled to PKWT	$V_{OXZ} = 23.6$ $V_{MHD} = 36.2$ $\theta_{V,OXZ} = \theta_{V,MHD} = 0.57$	$CL_{OXZ} = 188$ $CL_{MHD} = 3.09$ $\theta_{CL,OXZ} = 0.98$ $\theta_{CL,MHD} = 0.67$	6699.87	*Yes*	Yes	• $\omega_{V,MHD}$ decreased to 91%
M4	M3b	WT (Volume), PKWT (CL)	$\theta_{CL,OXZ}$ fixed to 1	$V_{OXZ} = 23.5$ $V_{MHD} = 36.5$ $\theta_{V,OXZ} = \theta_{V,MHD} = 0.58$	$CL_{OXZ} = 188$ $CL_{MHD} = 3.09$ $\theta_{CL,OXZ} = 1^f$ $\theta_{CL,MHD} = 0.67$	6697.90	*Yes*	Yes	• $\omega_{V,MHD}$ remained at 91% • High condition number (1681)
M5	M4	WT (Volume), PKWT (CL)	V_{MHD} fixed to 50	$V_{OXZ} = 30$ $V_{MHD} = 50^f$ $\theta_{V,OXZ} = \theta_{V,MHD} = 0.65$	$CL_{OXZ} = 221$ $CL_{MHD} = 3.05$ $\theta_{CL,OXZ} = 1^f$ $\theta_{CL,MHD} = 0.67$	6698.34	No	Yes	• $\omega_{V,MHD}$ decreased to 78% • Condition number 85

AIC, Akaike information criteria; CL, clearance of OXZ and MHD (as subscript); f , fixed value; θ, exponent of respective parameter mentioned in subscript; PKWT, Pharmacokinetic weight; RSE, relative standard error; V, volume of distribution of OXZ and MHD (as subscript); ω, between-subject variability of the respective parameter in subscript; WT, total body weight.

Table S3 (continued). Summary of selection of the scaler from WT and PKWT.

Model	Ref	PK scaler	Changes from the reference model	Fixed effects		AIC	AIC reduced?	Plausibility of estimates	Comment
				Volume of distribution (L)	Clearance (L/h)				
M5a	M5	WT (Volume), PKWT (CL)	Corr(V_{MHD}, CL_{MHD}) estimated (0.117)	$V_{OXZ} = 25.7$ $V_{MHD} = 50^{f}$ $\theta_{V,OXZ} = \theta_{V,MHD} = 0.69$	$CL_{OXZ} = 198$ $CL_{MHD} = 3.06$ $\theta_{CL,OXZ} = 1^{f}$ $\theta_{CL,MHD} = 0.67$	6695.48	Yes	Yes	• $\omega_{V,MHD}$ increased to 96% • Prolonged run time • Condition number 123
M6	M5	All scaled to PKWT	All scaled to PKWT	$V_{OXZ} = 33.1$ $V_{MHD} = 50^{f}$ $\theta_{V,OXZ} = \theta_{V,MHD} = 0.752$	$CL_{OXZ} = 220$ $CL_{MHD} = 3.05$ $\theta_{CL,OXZ} = 1^{f}$ $\theta_{CL,MHD} = 0.67$	6698.54	No	Yes	• $\omega_{V,MHD}$ 80% • Low run time • Condition number 44
M6a	M5	PKWT	Volume exponents fixed to 1, and V_{MHD} fixed to 50	$V_{OXZ} = 29.4$ $V_{MHD} = 50^{f}$ $\theta_{V,OXZ} = \theta_{V,MHD} = 1^{f}$	$CL_{OXZ} = 187$ $CL_{MHD} = 3.06$ $\theta_{CL,OXZ} = 1^{f}$ $\theta_{CL,MHD} = 0.67$	6695.87	Yes	Yes	• $\omega_{V,MHD}$ 104%

AIC, Akaike information criteria; CL, clearance of OXZ and MHD (as subscript); f, fixed value; θ, exponent of respective parameter mentioned in subscript; PKWT, Pharmacokinetic weight; RSE, relative standard error; V, volume of distribution of OXZ and MHD (as subscript); ω, between-subject variability of the respective parameter in subscript; WT, total body weight.

Table S4. Summary of two-compartment modeling.

Model	Ref	PK Scaler	Changes from the reference model	AIC	AIC Reduced?	Plausibility of Estimates	Comment
M7	M6	WT for volume and Q, PKWT for CL	Two compartment, All parameters estimated except $\theta_{CL,OXZ}$ fixed to 1	6697.47	Yes	Yes	• Abnormally high RSE% • $\omega_{V,MHD}$ increased to 125% • High run time • Unacceptable condition number (>10 log fold)
M7a	M6	WT for volume and Q, PKWT for CL	Two compartment, parameters fixed: $\theta_{CL,OXZ}$=1, $V_{OXZ} = 30$, $K_a = 0.25$, $CL_{OXZ} = 175$, $\theta_{CL,OXZ} = 1$, All volume exponents=0.65	6697.89	Yes	Yes	• $\omega_{V,MHD}$ increased to 95% • High run time • Unacceptable condition number (>8 log fold)
M7b	M6	WT for volume and Q, PKWT for CL	Two compartment, only one parameter fixed $V_{OXZ} = 30$	6697.50	Yes	Yes	• $\omega_{V,MHD}$ increased to 127% • High run time • Unacceptable condition number (>9 log fold)

AIC, Akaike information criteria; CL, clearance of OXZ and MHD (as subscript); f, fixed value; K_a, Absorption rate constant; θ, exponent of respective parameter mentioned in subscript; PKWT, Pharmacokinetic weight; Q, distribution clearance of MHD; RSE, relative standard error; V, volume of distribution of OXZ and MHD (as subscript); ω, between-subject variability of the respective parameter in subscript; WT, total body weight.

Table S5. Summary of covariate modeling.

Model #	Covariate	AIC
M6	PKWT	6698.54
M8a	PKWT + PNA	6699.51
M8b	PKWT + PMA (Hill)	6701.14
M9a	PKWT + SCR	6700.15
M9b	PKWT + eGFR	6701.47
M10a	PKWT + Phenobarbital	6700.34
M10b	PKWT + Valproic acid	6700.34
M10c	PKWT + Levetiracetam	6700.34
M10d	PKWT + Topiramate	6700.34

AIC, Akaike information criteria; eGFR, estimated glomerular filtration rate; PKWT, Pharmacokinetic weight; PNA, Post-natal age; SCR, Serum creatinine.

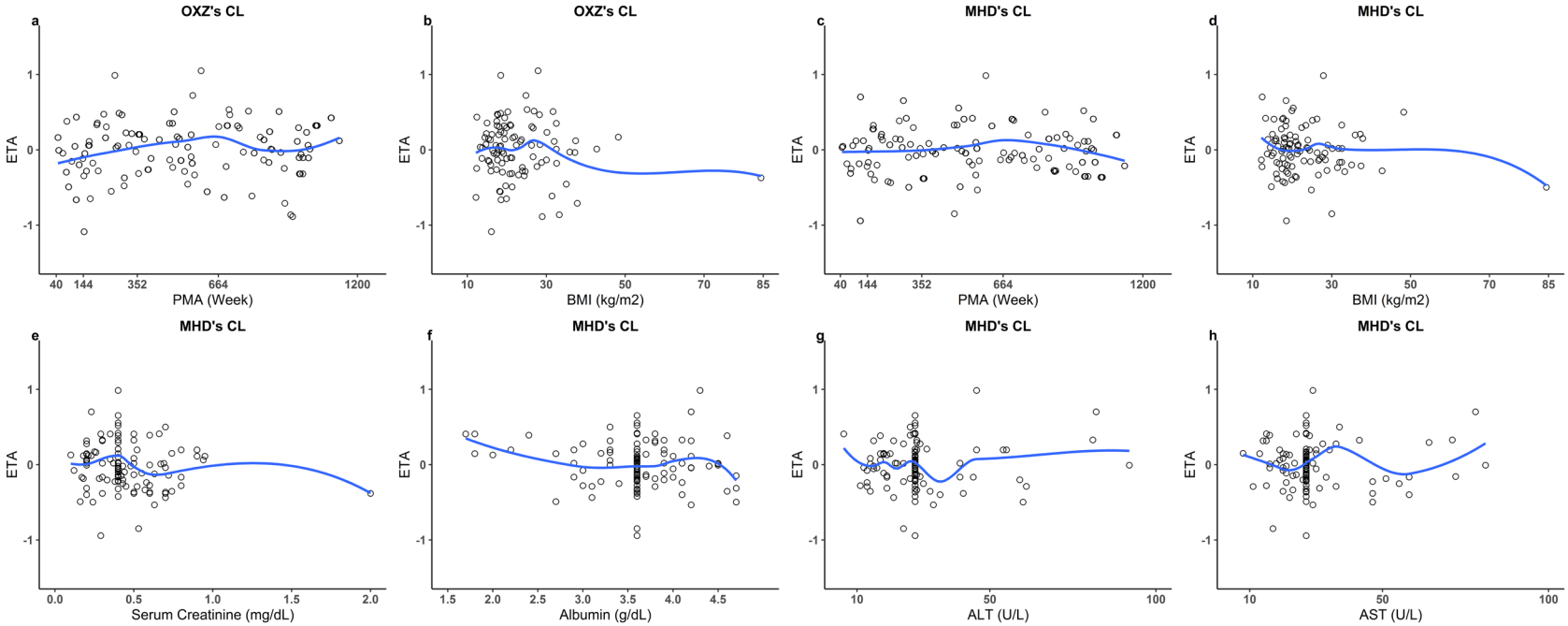

Figure S4. Empirical Bayesian Estimates of the between-subject effects (ETA) vs. continuous covariate from the model M6.

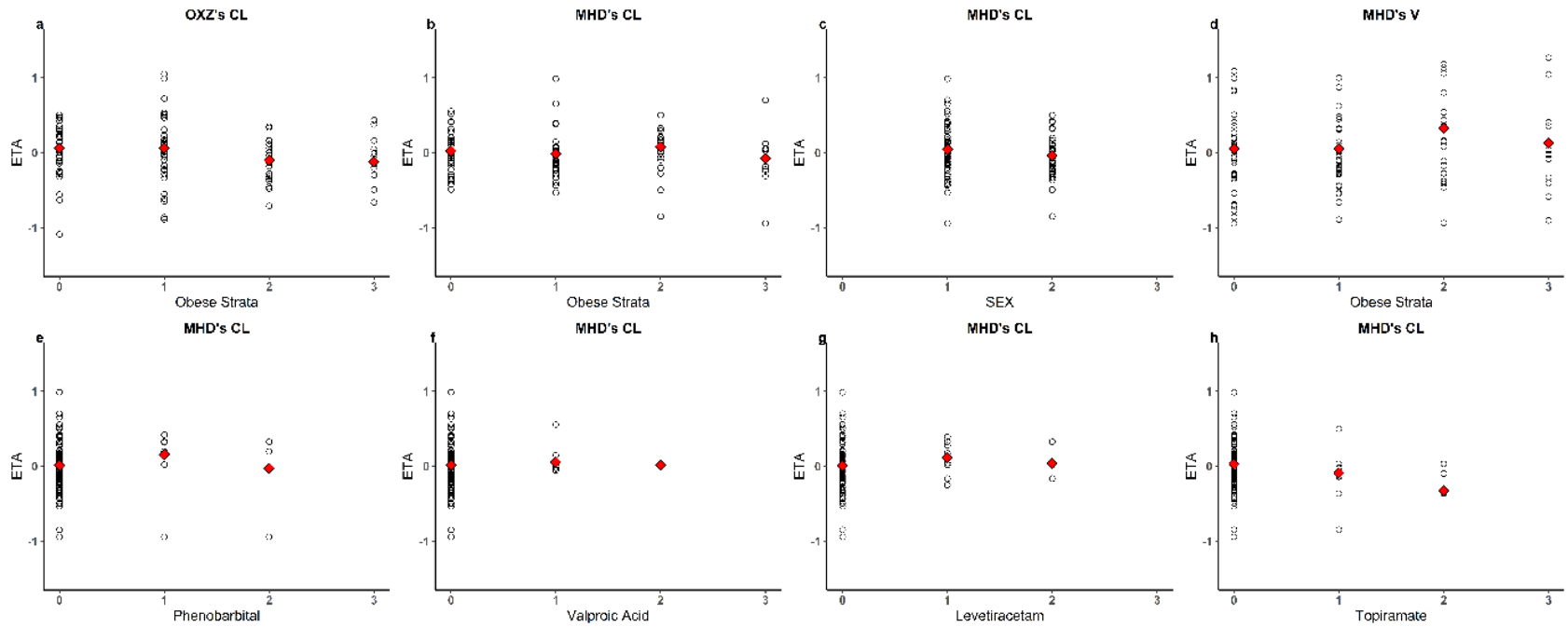

Figure S5. Empirical Bayesian Estimates of the between -subject effects (ETA) vs. categorical covariate from the model M6.

The red diamonds represent the mean value under each category; Obese strata: 0=not obese, 1=obese, 2=morbidly obese and 3=missing (<2 years); Co-medication strata: 0=not administered, 1=administered at a same day, 2= administered at a prior day and 3=unknown.

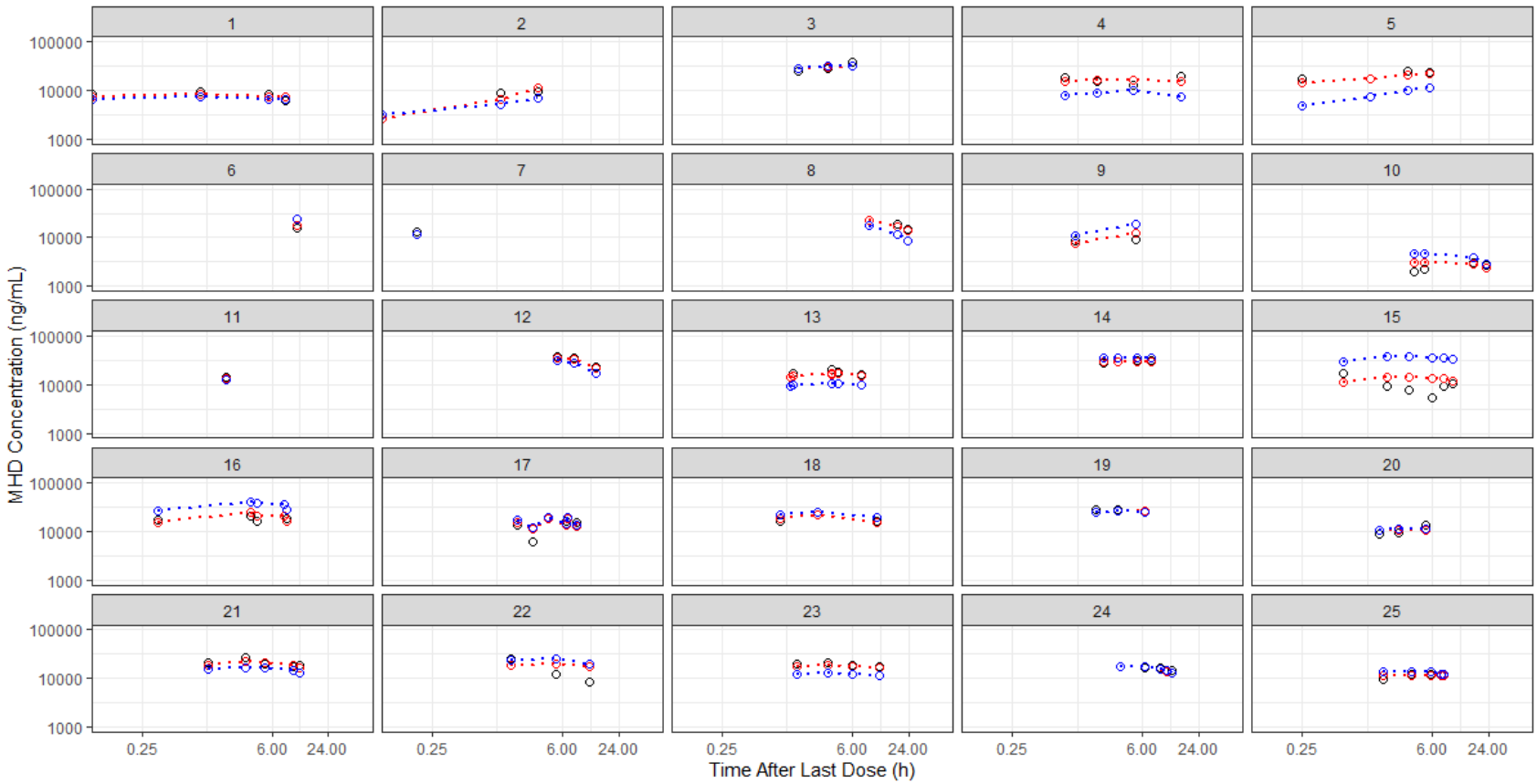

Figure S6. Individual predictions of MHD from PKWT model (M6) from ID1-ID25.

The observed, population predicted, and individual predicted concentrations are shown in black, blue, and red color respectively. The x-axis and y-axis are shown in logarithmic scale for better visualization. MHD, 10-mono-hydroxy derivative; PKWT, pharmacokinetic weight.

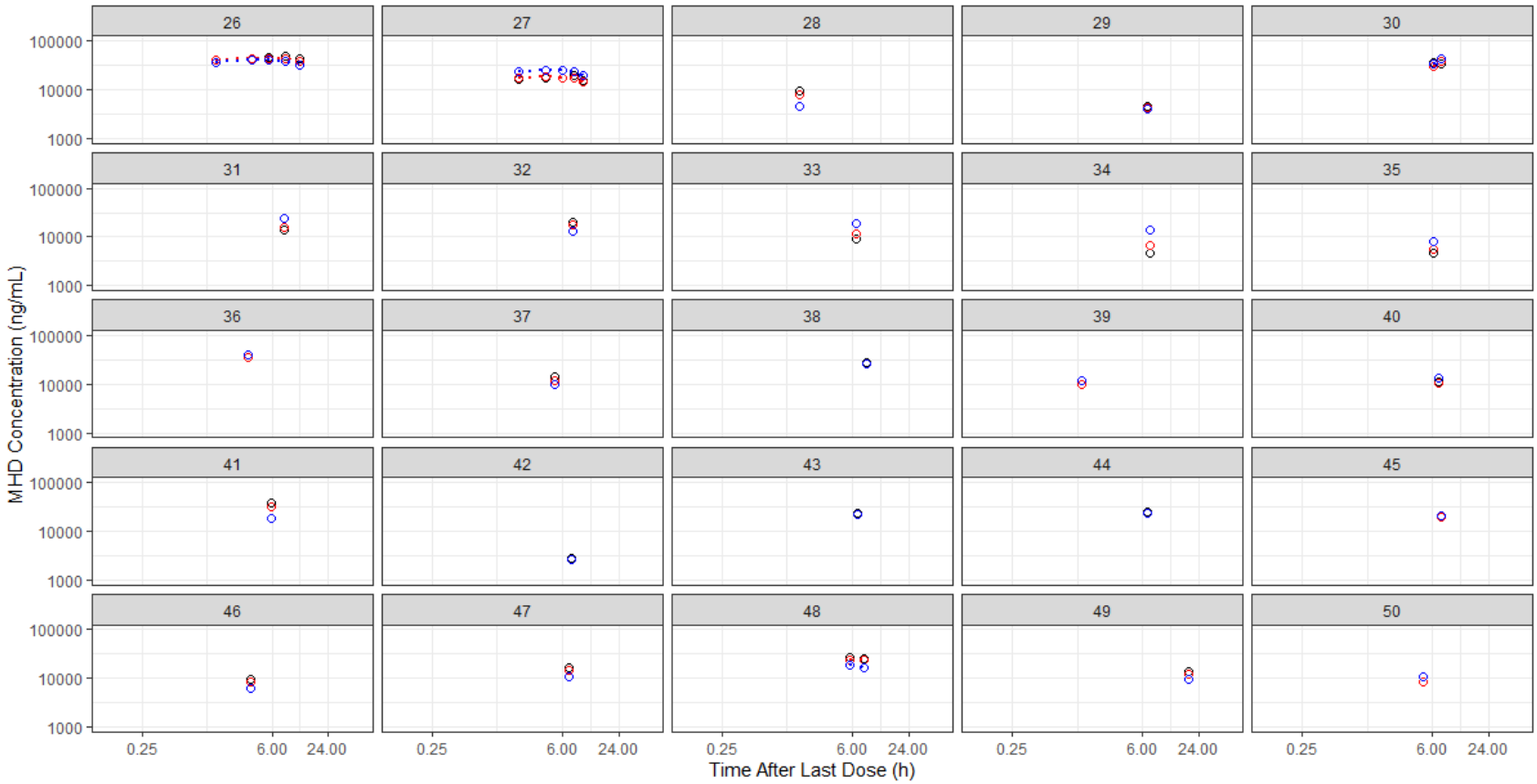

Figure S7. Individual predictions of MHD from PKWT model (M6) from ID26-ID50.

The observed, population predicted, and individual predicted concentrations are shown in black, blue, and red color respectively. The x-axis and y-axis are shown in logarithmic scale for better visualization. MHD, 10-mono-hydroxy derivative; PKWT, pharmacokinetic weight.

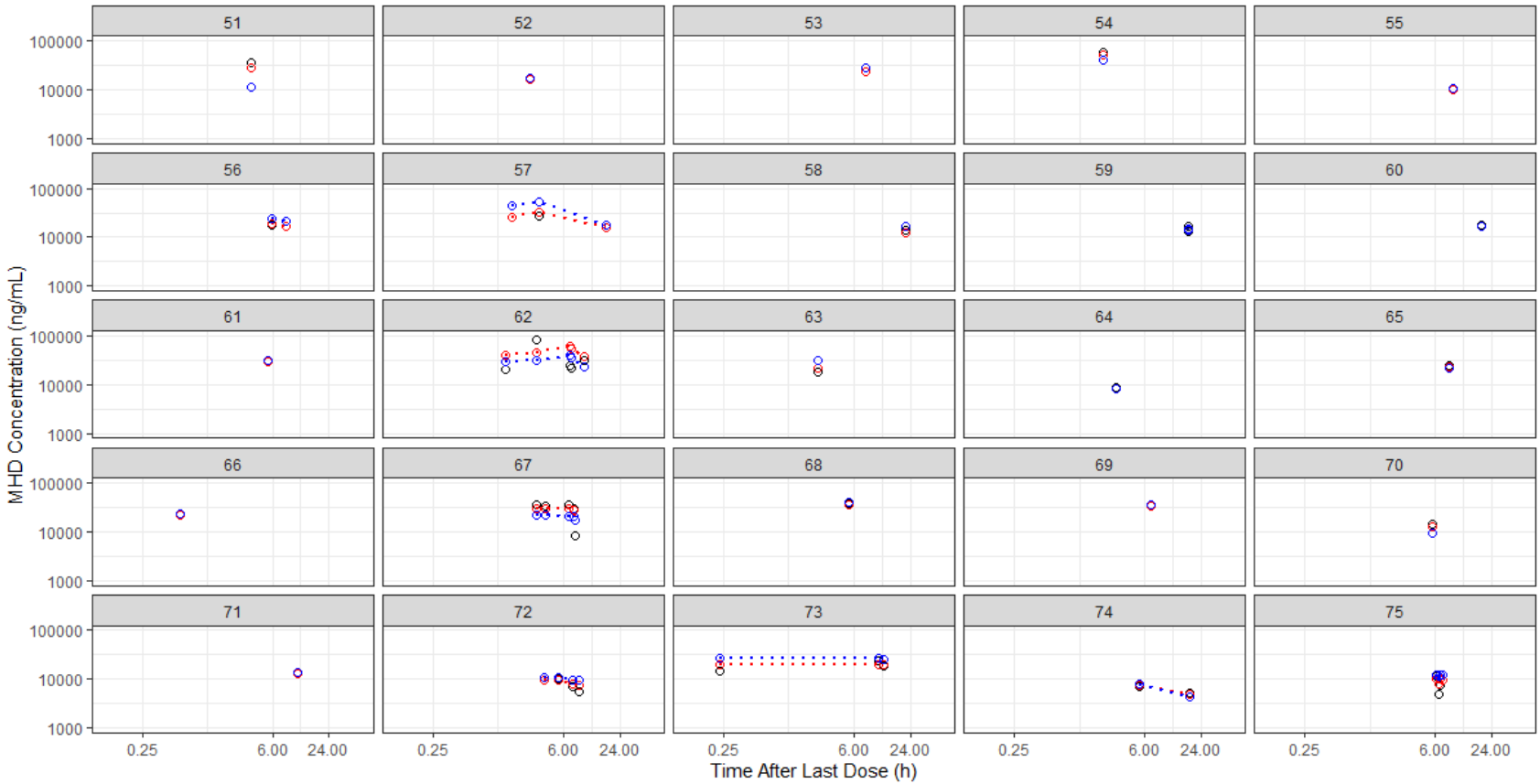

Figure S8. Individual predictions of MHD from PKWT model (M6) from ID51-ID75.

The observed, population predicted, and individual predicted concentrations are shown in black, blue, and red color respectively. The x-axis and y-axis are shown in logarithmic scale for better visualization. MHD, 10-mono-hydroxy derivative; PKWT, pharmacokinetic weight.

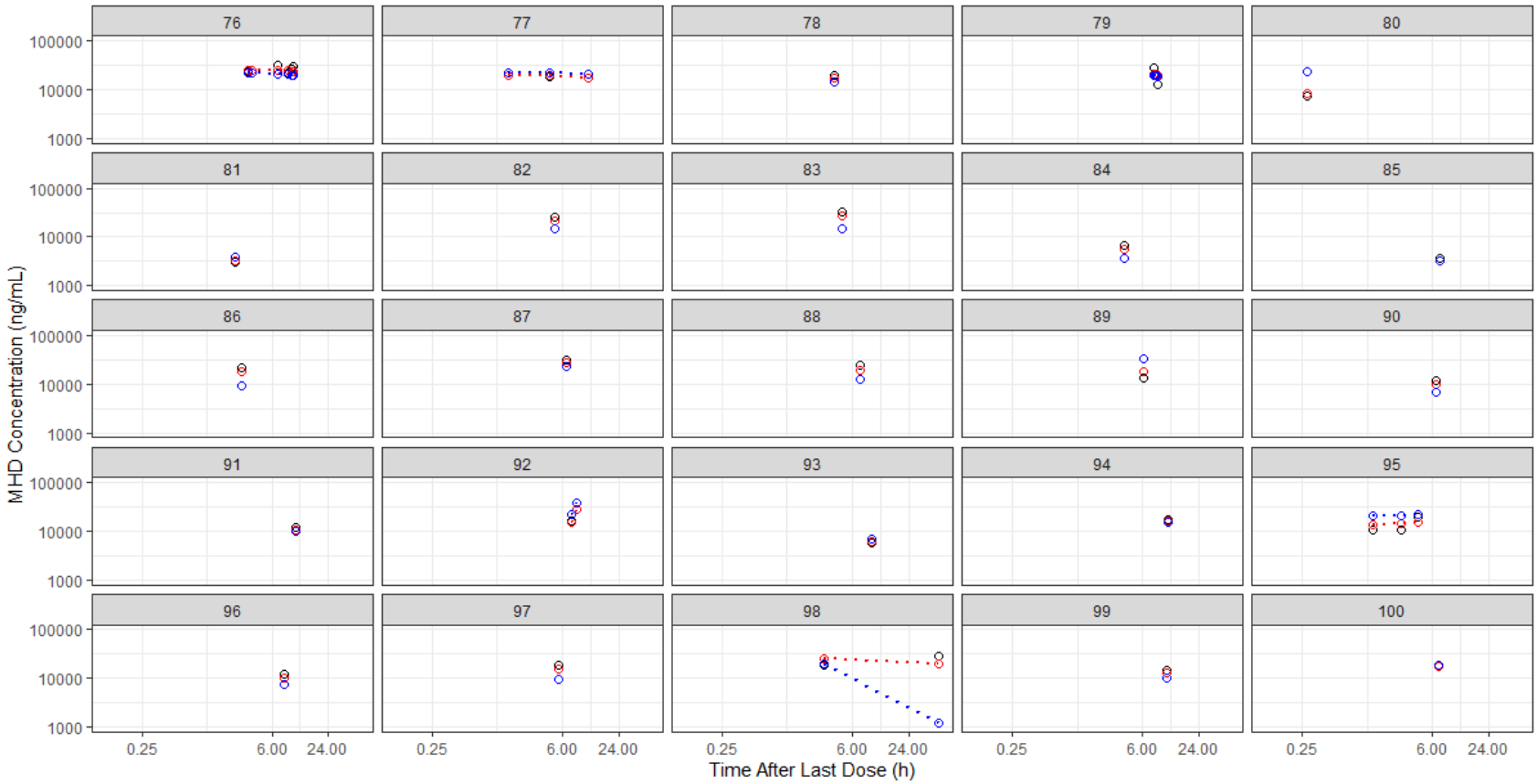

Figure S9. Individual predictions of MHD from PKWT model (M6) from ID76-ID100.

The observed, population predicted, and individual predicted concentrations are shown in black, blue, and red color respectively. The x-axis and y-axis are shown in logarithmic scale for better visualization. MHD, 10-mono-hydroxy derivative; PKWT, pharmacokinetic weight.

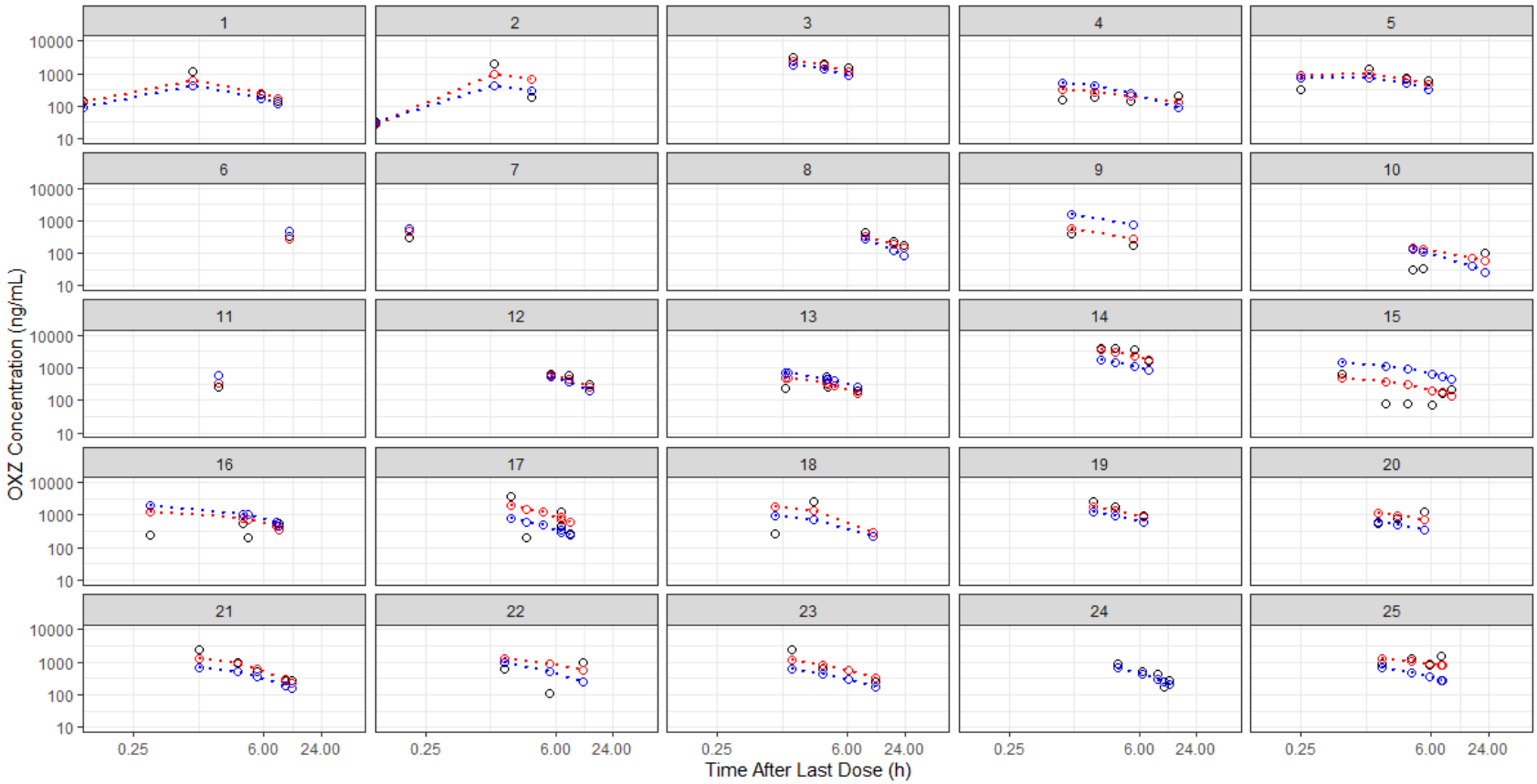

Figure S10. Individual predictions of OXZ from PKWT model (M6) from ID1-ID25.

The observed, population predicted, and individual predicted concentrations are shown in black, blue, and red color respectively. The x-axis and y-axis are shown in logarithmic scale for better visualization. OXZ, oxcarbazepine; PKWT, pharmacokinetic weight.

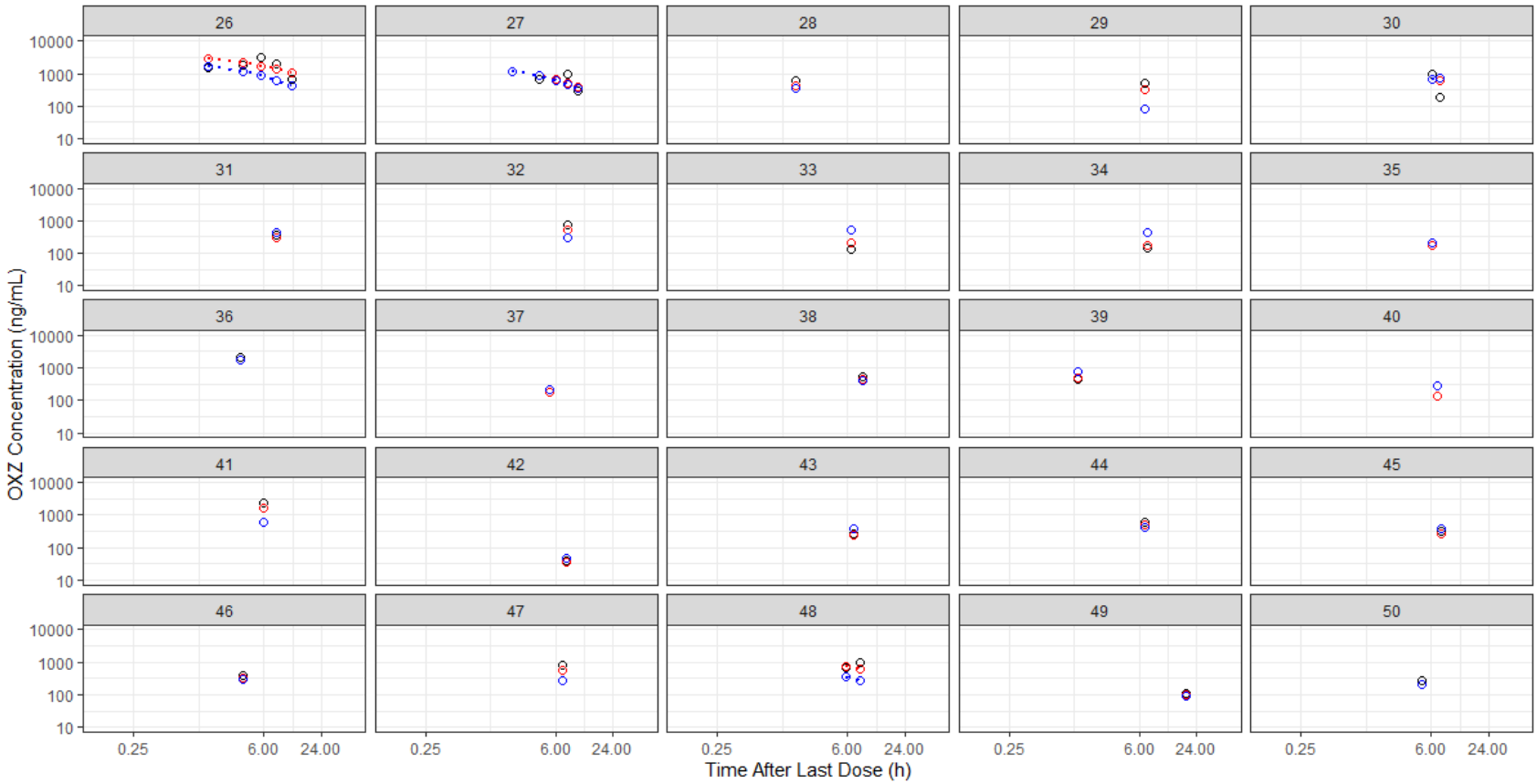

Figure S11. Individual predictions of OXZ from PKWT model (M6) from ID26-ID50.

The observed, population predicted, and individual predicted concentrations are shown in black, blue, and red color respectively. The x-axis and y-axis are shown in logarithmic scale for better visualization. OXZ, oxcarbazepine; PKWT, pharmacokinetic weight.

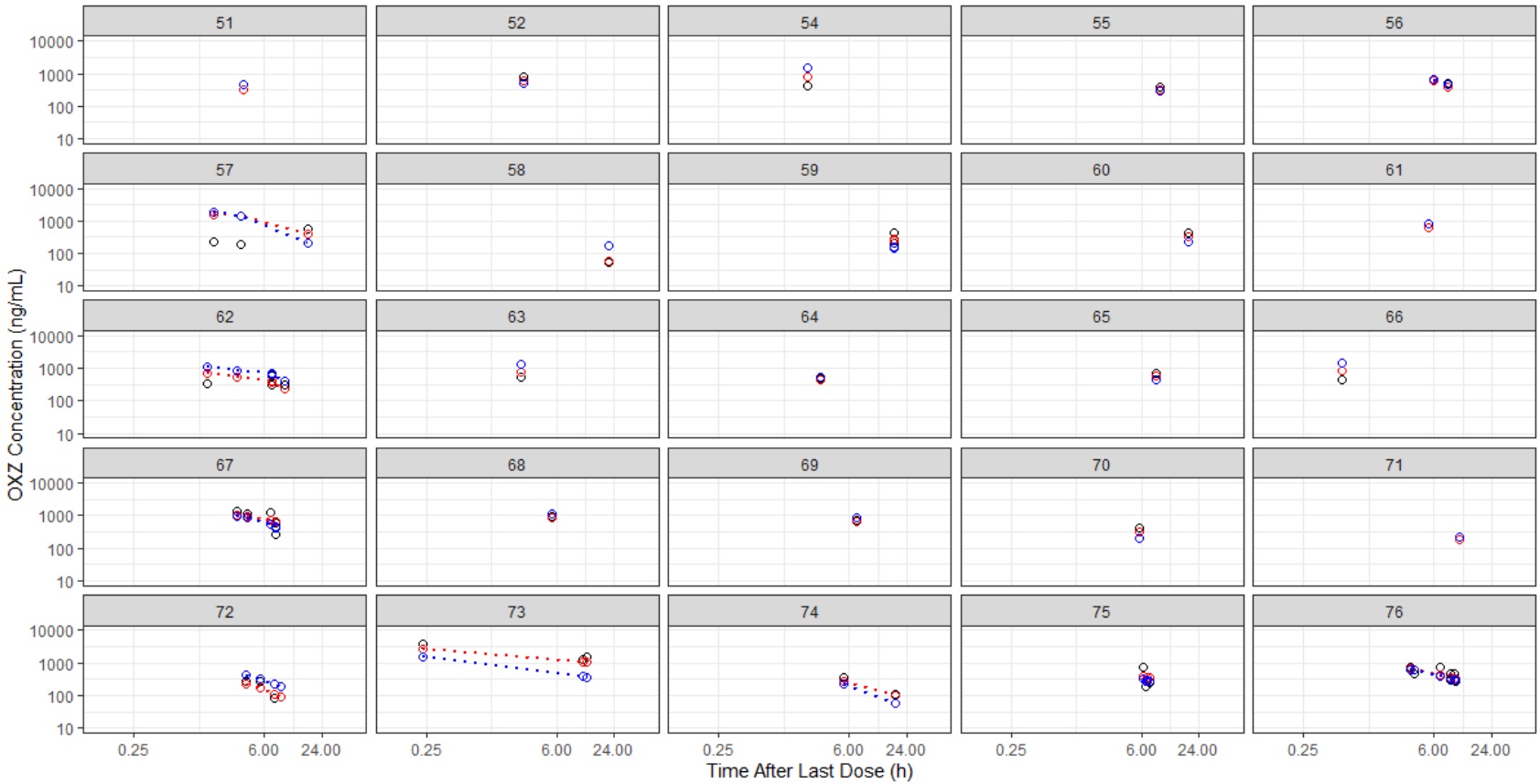

Figure S12. Individual predictions of OXZ from PKWT model (M6) from ID51-ID76.

The observed, population predicted, and individual predicted concentrations are shown in black, blue, and red color respectively. The x-axis and y-axis are shown in logarithmic scale for better visualization. OXZ, oxcarbazepine; PKWT, pharmacokinetic weight.

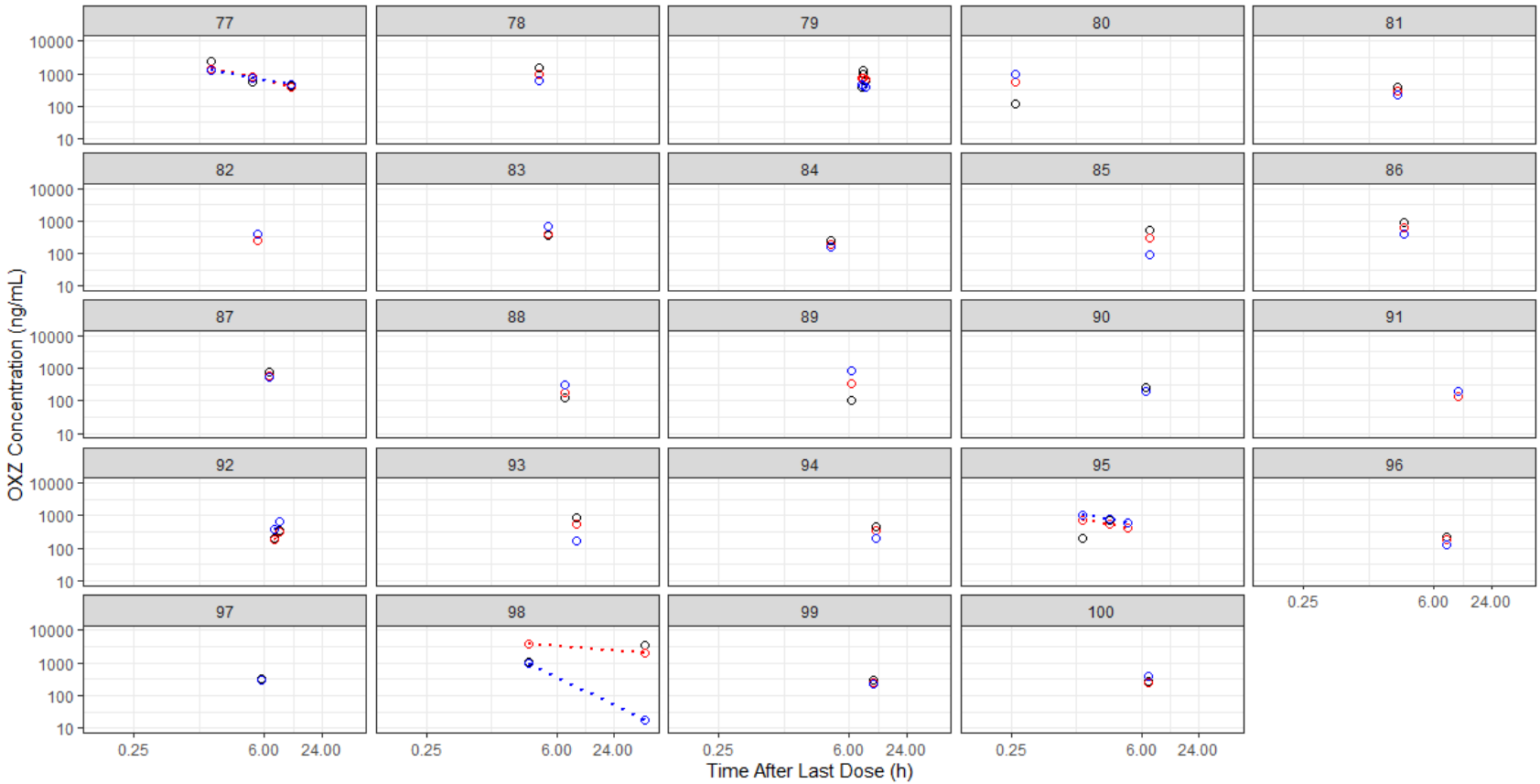

Figure S13. Individual predictions of OXZ from PKWT model (M6) from ID77-ID100.

The observed, population predicted, and individual predicted concentrations are shown in black, blue, and red color respectively. The x-axis and y-axis are shown in logarithmic scale for better visualization. OXZ, oxcarbazepine; PKWT, pharmacokinetic weight.

References

1. Janmahasatian S, et al. Quantification of lean bodyweight. Clinical pharmacokinetics. 2005;44:1051-65.
2. Al-Sallami HS, et al. Prediction of fat-free mass in children. Clinical pharmacokinetics. 2015;54:1169-78.
3. Centers for Disease Control and Prevention (CDC). National Center for Health Statistics (NCHS). National Health and Nutrition Examination Survey (NHANES) 1999-2016. https://wwwn.cdc.gov/nchs/nhanes/default.aspx. Accessed on October 25, 2019.
4. Hornik CP, et al. Creation of a multicenter pediatric inpatient data repository derived from electronic health records. Appl Clin Inform. 2019;10:307-15.